

EVCtrl: Efficient Control Adapter for Visual Generation

Zixiang Yang^{1†}, Yue Ma^{2†✉}, Yinhan Zhang², Shanhui Mo, Dongrui Liu³, Linfeng Zhang^{3✉}
¹ UESTC ² HKUST ³ SJTU

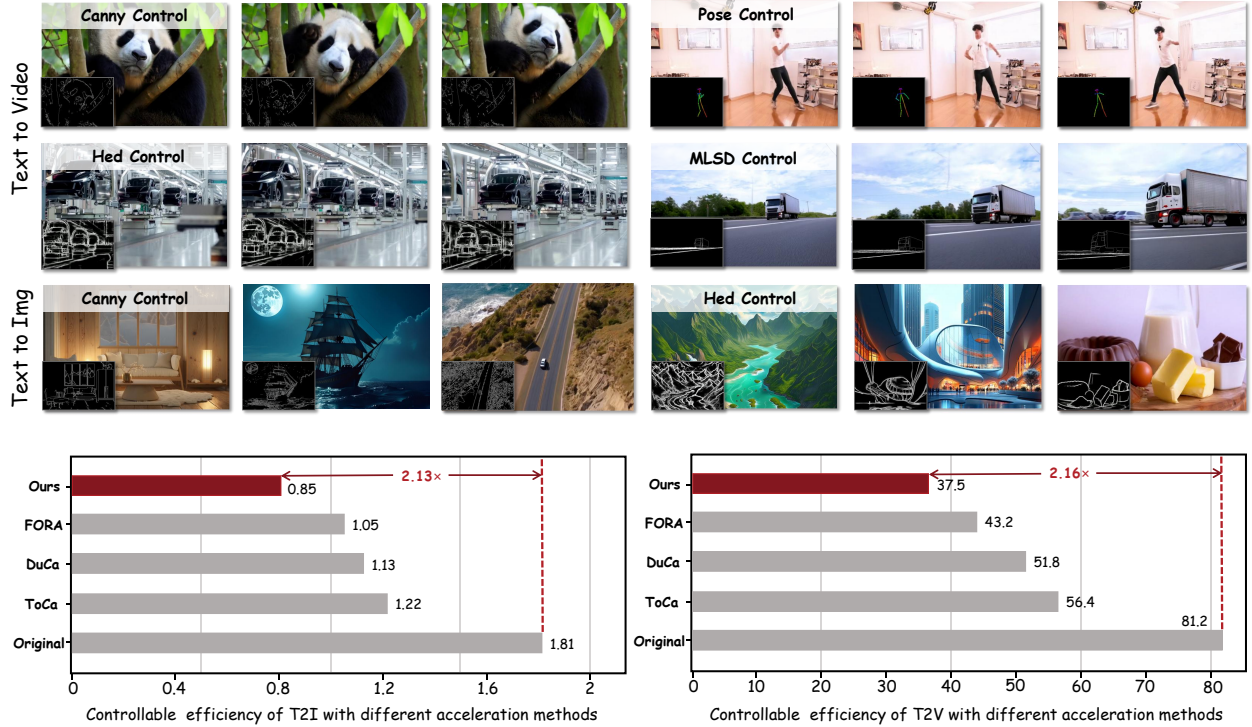


Figure 1. **Showcase of EVCtrl.** We propose the EVCtrl, a lightweight, plug-and-play control adapter. We present the outcomes of controllable image and video generation under various control conditions, along with an efficiency comparison.

Abstract

Visual generation includes both image and video generation, training probabilistic models to create coherent, diverse, and semantically faithful content from scratch. While early research focused on unconditional sampling, practitioners now demand controllable generation that allows precise specification of layout, pose, motion, or style. While ControlNet grants precise spatial-temporal control, its auxiliary branch markedly increases latency and introduces redundant computation in both uncontrolled regions and denoising steps, especially for video. To address this problem, we introduce **EVCtrl**, a lightweight, plug-and-play control adapter that slashes overhead without retraining the model. Specifically, we propose a spatio-temporal dual caching

strategy for sparse control information. **For spatial redundancy**, we first profile how each layer of DiT-ControlNet responds to fine-grained control, then partition the network into global and local functional zones. A locality-aware cache focuses computation on the local zones that truly need the control signal, skipping the bulk of redundant computation in global regions. **For temporal redundancy**, we selectively omit unnecessary denoising steps to improve efficiency. Extensive experiments on CogVideo-Controlnet, Wan2.1-Controlnet, and Flux demonstrate that our method is effective in image and video control generation without the need for training. For example, it achieves **2.16×** and **2.05×** speedups on CogVideo-Controlnet and Wan2.1-Controlnet, respectively, with almost no degradation in generation quality. Codes are available in the supplementary materials.

† Equal contribution.

✉ Corresponding author.

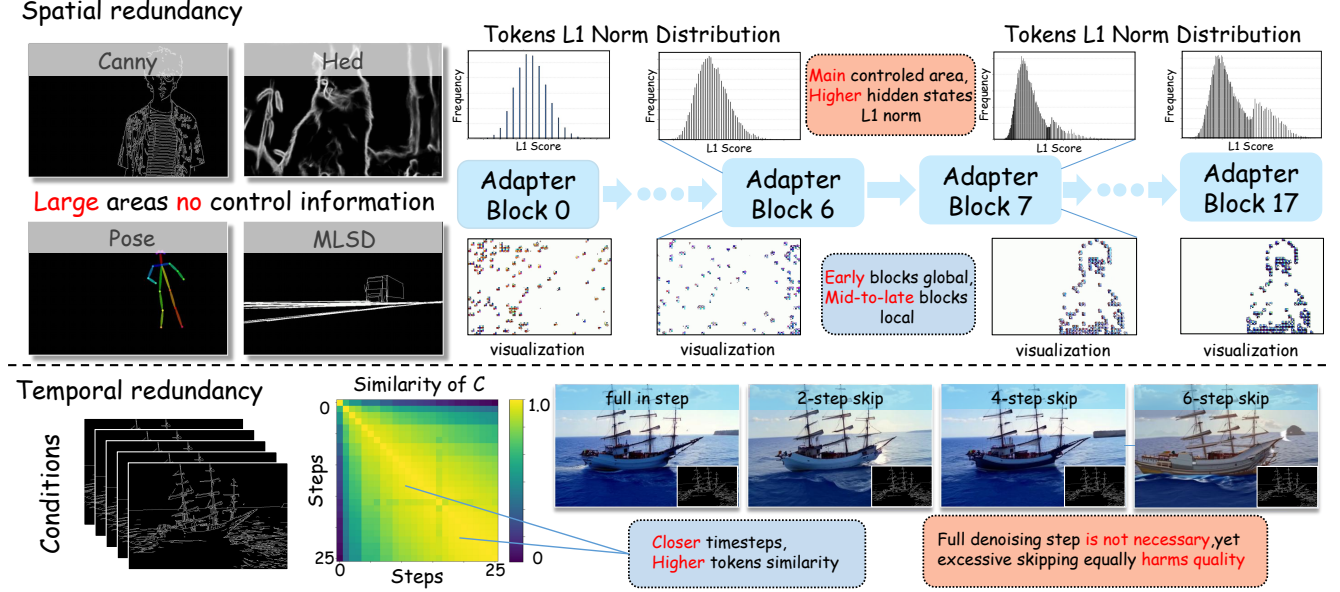


Figure 2. **Motivation illustration.** We observe significant spatial redundancy (a) and temporal redundancy (b) in controllable image and video generation. Spatially(a), large regions in the control image or video that carry no control information need not be computed. Temporally(b), skipping most highly similar adjacent diffusion timesteps does not impair controllability.

1. Introduction

Recent advances in the alignment of machine learning models for text-to-image [32, 37] and text-to-video synthesis [34–36, 38] have propelled a new wave of high-performance generators. Image models such as PixArt-delta[6], Stable Diffusion 3[10], Flux[1], Kolos[17], and Hunyuan-DiT[20], together with video models including Sora[25], CogVideoX[59], HunyuanVideo[18], and Qihoo-T2X[50], now deliver stunning visual fidelity and open up a wide spectrum of downstream applications.

However, current ControlNet-based[63] controlled generation methods for DiT have two major drawbacks. First, as an “auxiliary” neural network model structure, ControlNet typically directly replicates half of the network architecture, such as PixArt- δ [6], where a large number of additional parameters significantly increase the inference burden. Similarly, although OminiControl[46] only adds a limited number of parameters, it doubles the number of tokens involved in the attention and linear layers, resulting in an almost 70% increase in overall computational complexity. Second, during the entire diffusion process, the correlation between different time steps and the feature changes of conditional tokens is often overlooked, leading to low computational efficiency. To address these issues caused by computational complexity, this paper first examines the redundancy of conditional information in time and space:

Spatial Redundancy: We found that many spatial regions of conditional information are effectively empty, such as edgeless regions whose pixel values sit close to zero.

Tokens produced in these zones offer almost no guidance, yet the model still processes them, driving up computation without improving control fidelity. This inefficiency becomes most acute when the condition itself is sparse.

Temporal Redundancy: Figure 2 shows the distribution of the feature distances between adjacent time steps for different tokens, where a higher value indicates a lower similarity of the token between adjacent time steps. Observation reveals that conditional tokens C exhibit extremely high distances at most time steps during the diffusion process, while showing relatively low distances at individual time steps. This observation suggests that there is more significant temporal redundancy in Controlnet.

Motivated by these observations, we propose an **Efficient Visual Control Adapter(EVCtrl)**. For spatial redundancy, EVCtrl presents **Local Focused Caching(LFoC)**. LFoC identifies and stores only those tokens whose caching yields the highest benefit-to-cost ratio, prioritizing regions that encode salient edge cues. Concretely, during the denoising process, the adapter first computes and caches tokens across all spatial locations. In subsequent steps, tokens corresponding to edges are recomputed in full to preserve fidelity, whereas tokens associated with near-zero, edge-free regions are retrieved from the cache. This hybrid strategy enables the diffusion model to concentrate its capacity on edge-conditioned areas, sustaining control quality while substantially reducing computation over uniform regions.

Additionally, we observe temporal redundancy within the denoising processing: the conditioning signal evolves

unevenly across timesteps. EVCtrl’s **Denoising Step Skipping (DSS)** quantifies the dynamic variation of the condition at each step and retains full computation for the few timesteps that contribute most to the final control. By concentrating resources on these pivotal steps, DSS simultaneously lowers computational load and improves output quality. Numerous experiments in text-to-image and text-to-video generation have shown that EVCtrl is more effective than previous feature caching methods on CogVideo-Controlnet[47], Wan2.1-Controlnet, and Flux-Controlnet[57]. For example, on CogVideo-Controlnet[47], it can achieve $2.16\times$ acceleration, preserving near-lossless quality across various evaluation metrics when compared to the original controlnet pipeline without cache acceleration. In general, our contributions can be summarized as follows:

- We emphasize the spatial and temporal redundancies inherent to image and video generation tasks, and propose EVCtrl, a novel and efficient control adapter for controllable image and video generation.
- **Local Focused Caching (LFoC)**: To reduce spatial redundancy in the control signal, we propose spatial locality caching, which skips most computations over regions that receive no control. Then we identify the key carriers of fine-grained control information within DiT-ControlNet and construct a hierarchical attribution-sensitivity framework to further accelerate caching.
- **Denoising Step Skipping (DSS)**: To reduce temporal redundancy, we exploit the higher redundancy of the control branch relative to the original denoising path and the uneven influence of individual denoising steps on the conditioning signal, adaptively selecting the few steps that most affect the control for full computation while maintaining a periodic cache.
- Extensive experiments have been conducted on CogVideo-Controlnet, Wan2.1-Controlnet, and Flux-Controlnet, and the results show that EVCtrl achieves a high acceleration ratio while maintaining nearly lossless generation quality.

2. Related Works

2.1. Controllable Diffusion Models

To achieve conditional control in pre-trained text-to-image diffusion models, there are two main methods for introducing controllable conditions into image [56, 58, 61, 65, 66] or video generation models [31, 33]: (1) training a new large model from scratch for multi-condition compliance [15] (2) freezing the large pretrained model and fine-tuning only a lightweight adapter. Recent studies have extended these ideas to diffusion transformers (DiTs) [4, 5, 7, 12, 19, 39, 43, 45, 49, 51, 60], exploiting the built-in multimodal attention (MM-attention)[41] to inject image or video condi-

tions without further architectural change. T2I-Adapter[40] exemplifies the adapter route—it imposes minimal overhead yet yields weak control, limiting its use on complex prompts. In contrast, ControlNet[63] achieves stronger control effects by copying specific layers from pre-trained large models to guide image generation to align with control information, but it introduces a large number of additional parameters. Meanwhile, as the number of condition tokens increases, especially in controllable video generation, performing self-attention operations on the entire sequence of condition tokens leads to a significant increase in computational cost, imposing significant limitations on the controllable generation result rate from text to video.

2.2. Acceleration of Diffusion Models

Implementing low-latency and high-quality generation methods on diffusion models (DMs), including DiT, is an important research direction. Currently, there are mainly two types of acceleration methods for diffusion models: the first type is to reduce the number of sampling steps[8, 24, 26, 27, 44, 52, 67], and the second type is to accelerate the internal computation of diffusion models. Solutions to reduce computational complexity include model distillation and compression[55], token merging[2, 3, 11], token pruning[62], and layer-wise caching techniques[9, 13, 22, 29, 30, 42, 54]. However, layer-wise caching techniques use entire layers as the granularity and have difficulty perceiving the importance differences between tokens, resulting in key information being equally frozen or discarded. Toca[69] and Duca[70] instead use tokens as the minimum caching unit, accurately measure, and explicitly assign importance weights to each token with the help of a score map. In the subsequent computation stage, only high-weight tokens are refreshed according to a predetermined ratio, and the rest are directly reused from the cache, thus achieving lossless acceleration.

Unfortunately, the existing caching schemes are not specifically designed to adapt to ControlNet, which replicates specific layers in DM, and have the following issues: First, the existing caching and editing schemes often rely on explicit read and write operations of attention maps[69] or KV matrices[28, 68], which are incompatible with the mainstream Transformer acceleration pipeline and instead introduce additional latency. Additionally, there are differences in the correlation and importance of control information among different transformer layers in the existing diffusion transformer controlnet[5]. Meanwhile, the control conditions themselves provide prior information on the spatial distribution that should be focused on, but current methods fail to utilize these differences and information.

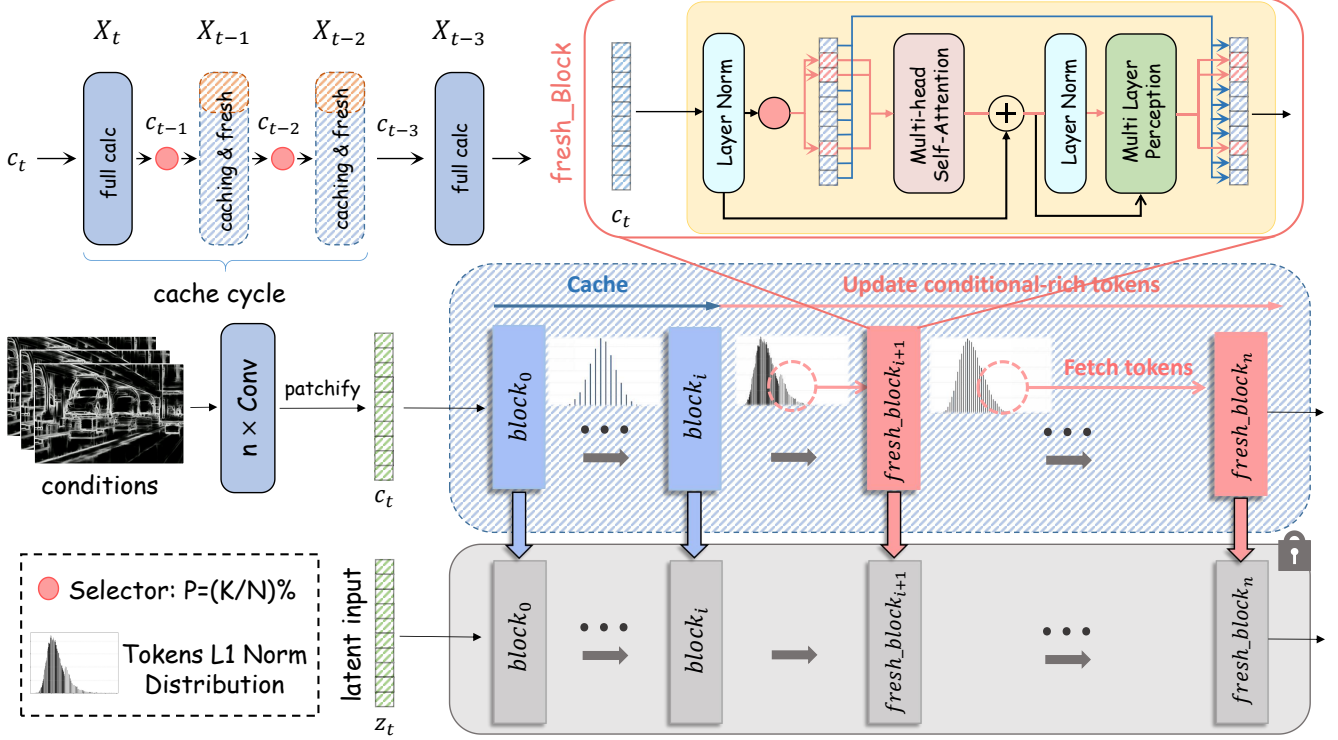


Figure 3. **Overall framework.** The pipeline takes initial noise and control conditions as inputs. Specifically, full caches are refreshed at fixed timestep intervals and at a handful of pivotal timesteps. For cached intermediate steps, only selected tokens within the mid-to-late fresh_blocks that capture local salient control cues are updated.

3. Method

3.1. Overall Framework

The pipeline of our method is shown in Figure 3. The core idea of EVCtrl is that, within each regular caching cycle, it performs full computation on an additional handful of denoising steps whose latent states critically determine the final output, while continuously updating the tokens that encode fine-grained control information, thereby mitigating errors introduced by repeatedly reusing stale control-signal features. In addition, existing caching strategies in deployed pipelines only cache the intermediate features of the MLP sub-layers inside a Transformer block. Unfortunately, the attention outputs themselves accumulate progressively larger errors when their outdated versions are reused, and these errors propagate downstream. Therefore, we extend the cache-update procedure to refresh the feature maps in both the attention and the MLP sub-layers simultaneously.

In the following, we first introduce the Spatial Locality Focused Caching to tackle the spatial redundancy within the Controlnet branch. Then we introduce the Temporal Denoising Step Skipping to tackle the temporal redundancy within the same branch.

3.2. Spatial Locality Focused Caching

3.2.1. Layer Sensitivity in DiT-ControlNet

To systematically characterise the layer-wise influence of DiT-ControlNet on both perceptual fidelity and conditional control accuracy, we propose a hierarchical attribution and sensitivity quantification framework that proceeds in three conceptually linked stages: norm-based observation, semantic mapping, and functional stratification. In the first stage, we extract every spatial token from the feature tensor produced by each DiT-ControlNet layer and compute its $L1$ norm. Global distributional properties are then estimated via histograms and kernel-density curves. In the second stage, a structure-similarity-driven alignment mechanism back-projects the indices of high-norm tokens into the original conditional domain, measuring their spatial overlap with the provided edge or pose guidance. This establishes an explicit correspondence between activation magnitude and fine-grained control semantics. Guided jointly by these two indicators, the network is stratified into two functional zones: (1) early layers exhibit peaked, low-variance distributions and are interpreted as robust encoders of low-frequency, global structural priors (2) mid-to-late layers display heavy-tailed distributions in which a minority of tokens obtain disproportionately large activations, thereby capturing

Table 1. **Quality and efficiency benchmarking results** of EVCtrl and other baselines

Type	Method	Quality					Efficiency	
		FID ↓	PSNR ↑	SSIM ↑	LPIPS ↓	VBench	Latency ↓	Speedup ↑
T2I	Flux-ControlNet (1024p)	–	–	–	–	–	1.81 s	1×
	+ Fora(N=2)	47.97	27.65	0.92	0.053	–	1.05 s	1.72×
	+ Toca(N=2)	55.82	26.98	0.90	0.065	–	1.22 s	1.48×
	+ Toca(N=4)	64.78	25.43	0.88	0.134	–	1.09 s	1.66×
	+ Taylorseer(N=2,O=4)	92.13	24.56	0.84	0.182	–	0.97 s	1.87×
	+ Ours(N=4)	34.69	28.74	0.94	0.042	–	0.93 s	1.95×
	+ Fora(N=4)	56.73	26.12	0.89	0.101	–	0.87 s	2.08×
	+ Taylorsser(N=4,O=4)	148.71	18.44	0.76	0.249	–	0.82 s	2.21×
	+ Ours(N=8)	42.34	27.88	0.91	0.057	–	0.85 s	2.13×
T2V	CogVideoX-ControlNet (480p, 6s, 48 frames)	–	–	–	–	82.6%	81.2 s	1×
	+ Fora(N=2)	51.45	23.55	0.83	0.13	82.2%	49.5 s	1.64×
	+ Toca(N=2)	62.97	20.93	0.78	0.18	81.6%	57.8 s	1.40×
	+ Toca(N=4)	71.34	18.84	0.75	0.21	79.8%	49.2 s	1.61×
	+ Taylorseer(N=2,O=4)	108.36	17.89	0.67	0.26	76.7%	46.4 s	1.75×
	+ Ours(N=4)	51.37	23.62	0.87	0.11	82.2%	43.4 s	1.88×
	+ Fora(N=4)	66.98	21.73	0.74	0.17	80.6%	40.1 s	2.02×
	+ Taylorsser(N=4,O=4)	160.48	14.97	0.53	0.38	72.9%	35.0 s	2.32×
	+ Ours(N=8)	64.83	22.13	0.81	0.15	81.3%	38.5 s	2.16×

ing high-frequency, local control cues such as edges, corners, and texture discontinuities. These high-energy tokens are identified as the primary carriers of fine-grained control information. This stratification paradigm is entirely training-free, providing an interpretable theoretical basis for subsequent selective caching strategies.

3.2.2. Spatial Token-wise Feature Caching

Analogous to prior token-wise conservative caching schemes, ToCa offers two attention map-based selection strategies, whereas Duca directly retains tokens whose value matrices exhibit small norms as surrogates for those receiving high attention scores, thereby neutralizing the incompatibility between attention-score-driven token selection and mainstream attention optimizers such as FlashAttention and other memory-efficient variants. However, these two token selection paradigms remain insufficiently tailored to the DiT-ControlNet architecture; therefore, we propose a markedly superior alternative to select conditional tokens.

Figure 2 empirically shows that tokens possessing large norms are strongly correlated with edge or pose conditioning signals. This observation motivates a caching strategy. It refreshes high-norm tokens more often within each interval. These tokens belong to mid-to-late layers that capture high-frequency local control cues and carry fine-grained information, thus strengthening conditional guid-

ance. The entire procedure can be inserted into any DiT-ControlNet inference pipeline without parameter modification or retraining, realizing fine-grained caching that “refreshes frequently where critical and sparingly where redundant.” Concretely, let P denote the proportion of critical conditional information; hence, the selection rule for \mathcal{P}_{Cache} is defined as follows:

$$\mathcal{P}_{Cache} = \arg \max_{\{i_1, i_2, \dots, i_n\} \subseteq \{1, 2, \dots, N\}} \{\|t_{i_1}\|_1, \|t_{i_2}\|_1, \dots, \|t_{i_n}\|_1\} \quad (1)$$

where the n is the total number of selected tokens, defined by $n = \lfloor P\% \times N \rfloor$

3.3. Temporal Denoising Step Skipping

3.3.1. Denoising Redundancy and Criticality Detection

After addressing spatial redundancy, we focus on the temporal redundancy that naturally emerges during iterative denoising in the control branch. As shown in Figure 2, we pairwise compare latent vectors across all timesteps through cosine similarity. Strikingly, tokens produced in consecutive denoising steps exhibit near-identical similarities, indicating an extremely slow evolution in latent space. This near-uniform behavior implies that substantial computational resources are repeatedly expended on nearly iden-

Table 2. **Quality and efficiency benchmarking results** of EVCtrl and other baselines across diverse control conditions

Method	Canny					Hed				
	Speed \uparrow	FID \downarrow	PSNR \uparrow	SSIM \uparrow	LPIPS \downarrow	Speed \uparrow	FID \downarrow	PSNR \uparrow	SSIM \uparrow	LPIPS \downarrow
+ Fora(N=4)	1.98 \times	64.85	22.74	0.75	0.16	1.97 \times	64.67	22.56	0.75	0.17
+ Toca(N=4)	1.55 \times	69.83	21.32	0.75	0.19	1.55 \times	69.74	21.25	0.76	0.18
+ Taylorseer(N=2)	1.85 \times	104.68	19.94	0.69	0.24	1.86 \times	104.59	19.92	0.69	0.25
+ Ours(N=8)	2.05 \times	62.24	23.26	0.80	0.12	2.02 \times	63.74	22.84	0.78	0.14

Method	Pose					MLSD				
	Speed \uparrow	FID \downarrow	PSNR \uparrow	SSIM \uparrow	LPIPS \downarrow	Speed \uparrow	FID \downarrow	PSNR \uparrow	SSIM \uparrow	LPIPS \downarrow
+ Fora(N=4)	1.98 \times	64.82	22.63	0.74	0.17	1.98 \times	64.79	22.68	0.75	0.16
+ Toca(N=4)	1.56 \times	69.81	21.31	0.75	0.19	1.55 \times	69.75	21.46	0.75	0.18
+ Taylorseer(N=2)	1.86 \times	104.47	19.86	0.70	0.22	1.87 \times	104.62	19.89	0.69	0.24
+ Ours(N=8)	2.23 \times	56.64	24.76	0.82	0.09	2.08 \times	60.31	23.83	0.81	0.11

tical representations. Meanwhile, although most adjacent denoising steps are highly redundant, Figure 2 also reveals abrupt drops in similarity at isolated timesteps. These sudden divergences mark rapid pivots in the denoising trajectory and inject details critical to final perceptual quality; consequently, these critical steps exert a disproportionately large influence on the final generation.

3.3.2. Stride-Skipping with Critical-Step Preservation

To take advantage of the inherent similarity between adjacent time steps more efficiently, without altering the underlying model architecture, we set a cache interval N . Features are fully recomputed and cached every N steps, then reused for the subsequent $N - 1$ timesteps. To prevent overly aggressive skipping from inadvertently discarding steps that significantly affect quality, we introduce a complementary mechanism: within each cache interval, critical steps identified a priori are selectively restored to full computation, ensuring essential details are preserved. Concretely, given a set of N adjacent timesteps $\{t, t - 1, \dots, t - (N - 1)\}$, we execute a full forward pass at the cycle’s leading timestep t to compute and store the features in a cache as $C_t^l := F(x_t^l)$, where the superscript $l \in \{1, 2, \dots, L\}$ denotes the layer index. Additionally, for a predetermined sequence of critical steps $\{k_0, k_1, \dots, k_m\}$, we assume a timestep k_i satisfies $t - 1 \leq k_i \leq t - (N - 1)$, $0 \leq i \leq m$. A full forward computation is executed at k_i to update the cache $C_{k_i}^l := F(x_{k_i}^l)$. The cached representation is then reused for all remaining redundant timesteps so that $F(\cdot)$ is not invoked again.

4. Experiments

4.1. Experimental Setups

4.1.1. Model Configurations

We conducted experiments with three commonly used DIT-based models equipped with ControlNet for various generative tasks, including Flux[57] for text-to-image generation, CogVideo[47], and Wan2.1[48] for text-to-video generation. The experiments were performed using an NVIDIA A800 80GB GPU. The CogVideo5B model is capable of generating 6-second videos with a resolution of 480p and a frame rate of 8fps. The Wan2.1-14B model can generate videos with a resolution of 720p or 480p, a frame rate of 16fps, and a duration of 5 seconds. Each model used its default sampling method: DPM-Solver++[27] with 20 steps for Flux, and DDIM[44] with 50 steps for both CogVideo and Wan2.1. For each model, we configure EVCtrl by setting the cache ratio P according to the redundancy level of the conditional information, while also employing various average forced-activation periods N .

4.1.2. Evaluation Protocol and Metrics.

We randomly selected 5,000 images and captions from the COCO-2017[21] dataset and extracted 100 videos and their descriptions from each of the 16 distinct categories of videos in the Vbench[16] dataset, totaling 1,600 videos. We evaluated the quality of the generated content using SSIM[53], LPIPS[64], PSNR[53], and FID[14]. Additionally, for text-to-video generation, we used video generation metrics within the Vbench framework as supplementary indicators.

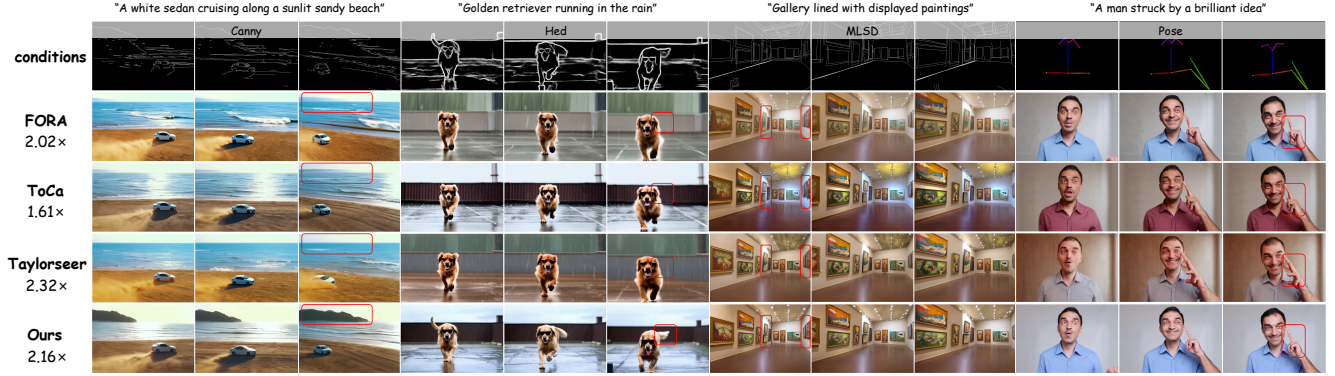


Figure 4. **The qualitative comparisons with existing methods.** Visualization comparing acceleration methods on Wan2.1-ControlNet: while others sacrifice control-condition details and introduce visual distortion at high speed-up ratios, ours preserves fine-grained details and maintains high-quality generation.

4.2. Comparison with baselines

4.2.1. Quantitative Results

As shown in Table 1, we benchmark EVCtrl against three state of the art training free acceleration baselines: ForA[42], Toca[69], and Taylorseer[23], on both the Flux-ControlNet[57] and CogVideo-ControlNet[47] pipelines. Quantitative results demonstrate that EVCtrl outperforms all other baselines across every quality metric (FID ↓, PSNR ↑, SSIM ↑, LPIPS ↓) while achieving equal or even higher acceleration ratios. Specifically, on the COCO2017 validation set at a $2.13\times$ speedup, EVCtrl achieves the lowest FID of 42.34 and maintains SSIM above 0.9; on the VBench validation set, it delivers a $2.16\times$ speedup with SSIM = 0.81, and all remaining metrics also surpass those of competing baselines at the same speedup, without any retraining or extra memory cost.

It is also noteworthy that as the caching period lengthens and the overall acceleration ratio continues to climb, the baseline methods suffer a sharp quality drop due to the loss of critical control signals during strided propagation: FID and LPIPS deteriorate rapidly, while PSNR and SSIM decline in tandem, leading to obvious artifacts or structural distortions in the generated images. By contrast, EVCtrl maintains exceptional adaptability; even when the caching period increases from $N = 4$ to $N = 8$, it still exhibits an unrivaled balance between efficiency and fidelity.

In addition, as summarized in Table 2, we evaluated EVCtrl in the Wan2.1-ControlNet pipeline under four distinct control modalities: Canny, HED, OpenPose, and MLSD. Quantitative results reveal that, regardless of the type of control, EVCtrl consistently outperforms all baselines on every quality metric (FID ↓, PSNR ↑, SSIM ↑, LPIPS ↓) while achieving equal or greater end-to-end acceleration. In particular, as the control signal becomes sparser, e.g., the thin edge maps produced by Canny or the minimal keypoint representation of OpenPose, the acceleration ratio

of EVCtrl rises further, reaching up to $2.4\times$ on OpenPose without any quality degradation. This trend confirms that EVCtrl is especially effective when the conditioning information is low-density, enabling it to skip redundant computation while still preserving fine-grained structural fidelity.

Table 3. **Ablation study on different configurations of LFoC and DSS** for controllable video generation

Method		Latency ↓	SSIM ↑	LPIPS ↓
LFoC-only	WA	37.6s	0.78	0.19
	WM	36.6s	0.74	0.22
DSS-only		35.8s	0.66	0.27
EVCtrl		39.2s	0.81	0.15

4.2.2. Qualitative Results

We compare EVCtrl with prior accelerators on Wan2.1-ControlNet under four control conditions (Canny, HED, MLSD, pose), highlighting its ability to accelerate inference while preserving controllable detail and video quality. The results are shown in 4. Across all conditions, EVCtrl consistently outperforms others in fidelity and detail: under Canny, it accurately reconstructs the distant mountains in the scene “a white sedan cruising along a sunlit sandy beach”; under HED, it retains the golden retriever’s tail in “golden retriever running in the rain”; under MLSD, it best matches the structural conditions in “gallery lined with displayed paintings”; and under pose guidance, the human hands exhibit both high quality and fidelity. In summary, EVCtrl leads existing methods in fidelity and detail.

4.3. Ablation Study

In the subsequent section, we will analyze the effectiveness of spatial module LFoC and temporal module DSS.

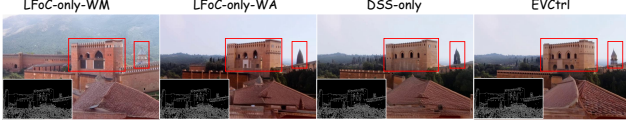


Figure 5. **The qualitative ablation study.** We select the canny as the input condition to ablate the performance.

4.3.1. Effectiveness of Local Focused Caching(LFoC)

Table 3 shows that removing LFoC lowers SSIM from 0.81 to 0.66 and raises LPIPS from 0.15 to 0.27, indicating a decline in generation quality. Moreover, comparing LFoC-with-attention(WA) and LFoC-with-MLP(WM) reveals that updating either the attention layers alone or the MLP layers alone leaves the cached key control tokens under-utilized. Only when LFoC refreshes both the attention and MLP layers simultaneously can the re-injected tokens fully unleash their expressive power, allowing the model to recover its original quality metrics. The visual results in Figure 5 demonstrate that after removing LFoC the model struggles to control fine details, illustrating that LFoC better exploits spatially local, fine-grained prior knowledge and achieves superior controllability in controlled generation tasks compared with the aggressive cache approach and the approach [69][70] that only updates the MLP layers.

4.3.2. Effectiveness of Denoising Step Skipping(DSS)

As shown in Table 3, DSS effectively shortens inference time with almost no loss in quality. Additionally, Table 1 demonstrates that DSS allows the skip interval N to be increased to 8 for reduced computational cost while maintaining the same or better controllable-generation performance as other acceleration methods achieve at only half that skip interval. Moreover, the visual results in Figure 5 reveal that removing DSS leads to a marked decline in both overall scene completeness and the fidelity of detail control, further validating the effectiveness and fidelity of our DSS strategy.

5. Conclusion

ControlNet-based controllable image and video generation usually incurs high computational costs due to spatial and temporal redundancies in diffusion models. To address this problem, we present EVCtrl, a training-free plug-and-play adapter that focuses computation on spatially local control-relevant tokens through spatial Local Focused Caching and prunes redundant denoising iterations through temporal Denoising Step Skipping. Extensive results demonstrate EVCtrl’s effectiveness for efficient controllable generation under diverse conditions. Our work offers valuable insights and directions toward future efficient, potentially real-time controllable image and video generation.

References

- [1] Black Forest Labs. Flux. <https://github.com/black-forest-labs/flux>, 2024. 2
- [2] Daniel Bolya and Judy Hoffman. Token merging for fast stable diffusion. In *Proceedings of the IEEE/CVF conference on computer vision and pattern recognition*, pages 4599–4603, 2023. 3
- [3] Daniel Bolya, Cheng-Yang Fu, Xiaoliang Dai, Peizhao Zhang, Christoph Feichtenhofer, and Judy Hoffman. Token merging: Your vit but faster. *arXiv preprint arXiv:2210.09461*, 2022. 3
- [4] Shengqu Cai, Eric Ryan Chan, Yunzhi Zhang, Leonidas Guibas, Jiajun Wu, and Gordon Wetzstein. Diffusion self-distillation for zero-shot customized image generation. In *Proceedings of the Computer Vision and Pattern Recognition Conference*, pages 18434–18443, 2025. 3
- [5] Ke Cao, Jing Wang, Ao Ma, Jiasong Feng, Zhanjie Zhang, Xuanhua He, Shanyuan Liu, Bo Cheng, Dawei Leng, Yuhui Yin, et al. Relactrl: Relevance-guided efficient control for diffusion transformers. *arXiv preprint arXiv:2502.14377*, 2025. 3
- [6] Junsong Chen, Yue Wu, Simian Luo, Enze Xie, Sayak Paul, Ping Luo, Hang Zhao, and Zhenguo Li. Pixart- δ : fast and controllable image generation with latent consistency models, 2024. 2
- [7] Qihua Chen, Yue Ma, Hongfa Wang, Junkun Yuan, Wenzhe Zhao, Qi Tian, Hongmei Wang, Shaobo Min, Qifeng Chen, and Wei Liu. Follow-your-canvas: Higher-resolution video outpainting with extensive content generation. *arXiv preprint arXiv:2409.01055*, 2024. 3
- [8] Siran Chen, Qinglin Xu, Yue Ma, Yu Qiao, and Yali Wang. Attentive snippet prompting for video retrieval. *IEEE Transactions on Multimedia*, 26:4348–4359, 2023. 3
- [9] Siran Chen, Yue Ma, Yu Qiao, and Yali Wang. M-bev: Masked bev perception for robust autonomous driving. In *Proceedings of the AAAI Conference on Artificial Intelligence*, pages 1183–1191, 2024. 3
- [10] Patrick Esser, Sumith Kulal, Andreas Blattmann, Rahim Entezari, Jonas Müller, Harry Saini, Yam Levi, Dominik Lorenz, Axel Sauer, Frederic Boesel, et al. Scaling rectified flow transformers for high-resolution image synthesis. In *Forty-first international conference on machine learning*, 2024. 2
- [11] Kunyu Feng, Yue Ma, Bingyuan Wang, Chenyang Qi, Haozhe Chen, Qifeng Chen, and Zeyu Wang. Dit4edit: Diffusion transformer for image editing. In *Proceedings of the AAAI Conference on Artificial Intelligence*, pages 2969–2977, 2025. 3
- [12] Kunyu Feng, Yue Ma, Xinhua Zhang, Boshi Liu, Yikuang Yuluo, Yinhan Zhang, Runtao Liu, Hongyu Liu, Zhiyuan Qin, Shanhui Mo, et al. Follow-your-instruction: A comprehensive mllm agent for world data synthesis. *arXiv preprint arXiv:2508.05580*, 2025. 3
- [13] Jiayi Gao, Kongming Liang, Tao Wei, Wei Chen, Zhanyu Ma, and Jun Guo. Dual-prior augmented decoding network for long tail distribution in hoi detection. In *Proceedings of*

- the AAAI Conference on Artificial Intelligence, pages 1806–1814, 2024. 3
- [14] Martin Heusel, Hubert Ramsauer, Thomas Unterthiner, Bernhard Nessler, and Sepp Hochreiter. Gans trained by a two time-scale update rule converge to a local nash equilibrium. *Advances in neural information processing systems*, 30, 2017. 6
- [15] Lianghai Huang, Di Chen, Yu Liu, Yujun Shen, Deli Zhao, and Jingren Zhou. Composer: Creative and controllable image synthesis with composable conditions. *arXiv preprint arXiv:2302.09778*, 2023. 3
- [16] Ziqi Huang, Yinan He, Jiashuo Yu, Fan Zhang, Chenyang Si, Yuming Jiang, Yuanhan Zhang, Tianxing Wu, Qingyang Jin, Nattapol Chanpaisit, et al. Vbench: Comprehensive benchmark suite for video generative models. In *Proceedings of the IEEE/CVF Conference on Computer Vision and Pattern Recognition*, pages 21807–21818, 2024. 6
- [17] Kolos Team. Kolos: Effective training of diffusion model for photorealistic text-to-image synthesis. *arXiv preprint*, 2024. 2
- [18] Weijie Kong, Qi Tian, Zijian Zhang, Rox Min, Zuozhuo Dai, Jin Zhou, Jiangfeng Xiong, Xin Li, Bo Wu, Jianwei Zhang, et al. Hunyuanvideo: A systematic framework for large video generative models. *arXiv preprint arXiv:2412.03603*, 2024. 2
- [19] Jiajun Li, Yue Ma, Xinyu Zhang, Qingyan Wei, Songhua Liu, and Linfeng Zhang. Skipvar: Accelerating visual autoregressive modeling via adaptive frequency-aware skipping. *arXiv preprint arXiv:2506.08908*, 2025. 3
- [20] Zhimin Li, Jianwei Zhang, Qin Lin, Jiangfeng Xiong, Yanxin Long, Xincheng Deng, Yingfang Zhang, Xingchao Liu, Minbin Huang, Zedong Xiao, Dayou Chen, Jiajun He, Jiahao Li, Wenyue Li, Chen Zhang, Rongwei Quan, Jianxiang Lu, Jiabin Huang, Xiaoyan Yuan, Xiaoxiao Zheng, Yixuan Li, Jihong Zhang, Chao Zhang, Meng Chen, Jie Liu, Zheng Fang, Weiyang Wang, Jinbao Xue, Yangyu Tao, Jianchen Zhu, Kai Liu, Sihuan Lin, Yifu Sun, Yun Li, Dongdong Wang, Mingtao Chen, Zhichao Hu, Xiao Xiao, Yan Chen, Yuhong Liu, Wei Liu, Di Wang, Yong Yang, Jie Jiang, and Qinglin Lu. Hunyuan-dit: A powerful multi-resolution diffusion transformer with fine-grained chinese understanding, 2024. 2
- [21] Tsung-Yi Lin, Michael Maire, Serge Belongie, James Hays, Pietro Perona, Deva Ramanan, Piotr Dollár, and C Lawrence Zitnick. Microsoft coco: Common objects in context. In *European conference on computer vision*, pages 740–755. Springer, 2014. 6
- [22] Haozhe Liu, Wentian Zhang, Jinheng Xie, Francesco Facio, Mengmeng Xu, Tao Xiang, Mike Zheng Shou, Juan-Manuel Perez-Rua, and Jürgen Schmidhuber. Faster diffusion via temporal attention decomposition. *arXiv preprint arXiv:2404.02747*, 2024. 3
- [23] Jiacheng Liu, Chang Zou, Yuanhuiyi Lyu, Junjie Chen, and Linfeng Zhang. From reusing to forecasting: Accelerating diffusion models with taylorseers. *arXiv preprint arXiv:2503.06923*, 2025. 7
- [24] Xingchao Liu, Chengyue Gong, and Qiang Liu. Flow straight and fast: Learning to generate and transfer data with rectified flow. *arXiv preprint arXiv:2209.03003*, 2022. 3
- [25] Yixin Liu, Kai Zhang, Yuan Li, Zhiling Yan, Chujie Gao, Ruoxi Chen, Zhengqing Yuan, Yue Huang, Hanchi Sun, Jianfeng Gao, Lifang He, and Lichao Sun. Sora: A review on background, technology, limitations, and opportunities of large vision models, 2024. 2
- [26] Cheng Lu, Yuhao Zhou, Fan Bao, Jianfei Chen, Chongxuan Li, and Jun Zhu. Dpm-solver: A fast ode solver for diffusion probabilistic model sampling in around 10 steps. *Advances in neural information processing systems*, 35:5775–5787, 2022. 3
- [27] Cheng Lu, Yuhao Zhou, Fan Bao, Jianfei Chen, Chongxuan Li, and Jun Zhu. Dpm-solver++: Fast solver for guided sampling of diffusion probabilistic models. *Machine Intelligence Research*, pages 1–22, 2025. 3, 6
- [28] Shilin Lu, Yanzhu Liu, and Adams Wai-Kin Kong. Tf-icon: Diffusion-based training-free cross-domain image composition. In *Proceedings of the IEEE/CVF International Conference on Computer Vision*, pages 2294–2305, 2023. 3
- [29] Xinyin Ma, Gongfan Fang, Michael Bi Mi, and Xinchao Wang. Learning-to-cache: Accelerating diffusion transformer via layer caching. *Advances in Neural Information Processing Systems*, 37:133282–133304, 2024. 3
- [30] Xinyin Ma, Gongfan Fang, and Xinchao Wang. Deepcache: Accelerating diffusion models for free. In *Proceedings of the IEEE/CVF conference on computer vision and pattern recognition*, pages 15762–15772, 2024. 3
- [31] Yue Ma, Yali Wang, Yue Wu, Ziyu Lyu, Siran Chen, Xiu Li, and Yu Qiao. Visual knowledge graph for human action reasoning in videos. In *Proceedings of the 30th ACM International Conference on Multimedia*, pages 4132–4141, 2022. 3
- [32] Yue Ma, Xiaodong Cun, Yingqing He, Chenyang Qi, Xintao Wang, Ying Shan, Xiu Li, and Qifeng Chen. Magicstick: Controllable video editing via control handle transformations. *arXiv preprint arXiv:2312.03047*, 2023. 2
- [33] Yue Ma, Yingqing He, Xiaodong Cun, Xintao Wang, Siran Chen, Xiu Li, and Qifeng Chen. Follow your pose: Pose-guided text-to-video generation using pose-free videos. In *Proceedings of the AAAI Conference on Artificial Intelligence*, pages 4117–4125, 2024. 3
- [34] Yue Ma, Hongyu Liu, Hongfa Wang, Heng Pan, Yingqing He, Junkun Yuan, Ailing Zeng, Chengfei Cai, Heung-Yeung Shum, Wei Liu, et al. Follow-your-emoji: Fine-controllable and expressive freestyle portrait animation. In *SIGGRAPH Asia 2024 Conference Papers*, pages 1–12, 2024. 2
- [35] Yue Ma, Kunyu Feng, Zhongyuan Hu, Xinyu Wang, Yucheng Wang, Mingzhe Zheng, Xuanhua He, Chenyang Zhu, Hongyu Liu, Yingqing He, et al. Controllable video generation: A survey. *arXiv preprint arXiv:2507.16869*, 2025.
- [36] Yue Ma, Kunyu Feng, Xinhua Zhang, Hongyu Liu, David Junhao Zhang, Jinbo Xing, Yinhan Zhang, Ayden Yang, Zeyu Wang, and Qifeng Chen. Follow-your-creation: Empowering 4d creation through video inpainting. *arXiv preprint arXiv:2506.04590*, 2025. 2
- [37] Yue Ma, Yingqing He, Hongfa Wang, Andong Wang, Leqi Shen, Chenyang Qi, Jixuan Ying, Chengfei Cai, Zhifeng Li,

- Heung-Yeung Shum, et al. Follow-your-click: Open-domain regional image animation via motion prompts. In *Proceedings of the AAAI Conference on Artificial Intelligence*, pages 6018–6026, 2025. 2
- [38] Yue Ma, Yulong Liu, Qiyuan Zhu, Ayden Yang, Kunyu Feng, Xinhua Zhang, Zhifeng Li, Sirui Han, Chenyang Qi, and Qifeng Chen. Follow-your-motion: Video motion transfer via efficient spatial-temporal decoupled finetuning. *arXiv preprint arXiv:2506.05207*, 2025. 2
- [39] Chaojie Mao, Jingfeng Zhang, Yulin Pan, Zeyinzi Jiang, Zhen Han, Yu Liu, and Jingren Zhou. Ace++: Instruction-based image creation and editing via context-aware content filling. *arXiv preprint arXiv:2501.02487*, 2025. 3
- [40] Chong Mou, Xintao Wang, Liangbin Xie, Yanze Wu, Jian Zhang, Zhongang Qi, and Ying Shan. T2i-adapter: Learning adapters to dig out more controllable ability for text-to-image diffusion models. In *Proceedings of the AAAI conference on artificial intelligence*, pages 4296–4304, 2024. 3
- [41] Zexu Pan, Zhaojie Luo, Jichen Yang, and Haizhou Li. Multi-modal attention for speech emotion recognition. *arXiv preprint arXiv:2009.04107*, 2020. 3
- [42] Pratheba Selvaraju, Tianyu Ding, Tianyi Chen, Ilya Zharkov, and Luming Liang. Fora: Fast-forward caching in diffusion transformer acceleration. *arXiv preprint arXiv:2407.01425*, 2024. 3, 7
- [43] D She, Mushui Liu, Jingxuan Pang, Jin Wang, Zhen Yang, Wanggui He, Guanghao Zhang, Yi Wang, Qihan Huang, Haobin Tang, et al. Customvideox: 3d reference attention driven dynamic adaptation for zero-shot customized video diffusion transformers. *arXiv preprint arXiv:2502.06527*, 2025. 3
- [44] Jiaming Song, Chenlin Meng, and Stefano Ermon. Denoising diffusion implicit models. *arXiv preprint arXiv:2010.02502*, 2020. 3, 6
- [45] Zhenxiong Tan, Songhua Liu, Xingyi Yang, Qiaochu Xue, and Xinchao Wang. Ominicontrol: Minimal and universal control for diffusion transformer. *arXiv preprint arXiv:2411.15098*, 2024. 3
- [46] Zhenxiong Tan, Songhua Liu, Xingyi Yang, Qiaochu Xue, and Xinchao Wang. Ominicontrol: Minimal and universal control for diffusion transformer. 2025. 2
- [47] TheDenk. Cogvideo controlnet. <https://github.com/TheDenk/cogvideox-controlnet>, 2024. 3, 6, 7
- [48] Team Wan, Ang Wang, Baole Ai, Bin Wen, Chaojie Mao, Chen-Wei Xie, Di Chen, Feiwu Yu, Haiming Zhao, Jianxiao Yang, et al. Wan: Open and advanced large-scale video generative models. *arXiv preprint arXiv:2503.20314*, 2025. 6
- [49] Zhen Wan, Yue Ma, Chenyang Qi, Zhiheng Liu, and Tao Gui. Unipaint: Unified space-time video inpainting via mixture-of-experts. *arXiv preprint arXiv:2412.06340*, 2024. 3
- [50] Jing Wang, Ao Ma, Jiasong Feng, Dawei Leng, Yuhui Yin, and Xiaodan Liang. Qihoo-t2x: An efficient proxy-tokenized diffusion transformer for text-to-any-task, 2024. 2
- [51] Jiangshan Wang, Yue Ma, Jiayi Guo, Yicheng Xiao, Gao Huang, and Xiu Li. Cove: Unleashing the diffusion feature correspondence for consistent video editing. *arXiv preprint arXiv:2406.08850*, 2024. 3
- [52] Jiangshan Wang, Junfu Pu, Zhongang Qi, Jiayi Guo, Yue Ma, Nisha Huang, Yuxin Chen, Xiu Li, and Ying Shan. Taming rectified flow for inversion and editing. *arXiv preprint arXiv:2411.04746*, 2024. 3
- [53] Zhou Wang, Alan C Bovik, Hamid R Sheikh, and Eero P Simoncelli. Image quality assessment: from error visibility to structural similarity. *IEEE transactions on image processing*, 13(4):600–612, 2004. 6
- [54] Yicheng Xiao, Yue Ma, Shuyan Li, Hantao Zhou, Ran Liao, and Xiu Li. Semanticac: semantics-assisted framework for audio classification. In *ICASSP 2023-2023 IEEE International Conference on Acoustics, Speech and Signal Processing (ICASSP)*, pages 1–5. IEEE, 2023. 3
- [55] Enze Xie, Junsong Chen, Junyu Chen, Han Cai, Haotian Tang, Yujun Lin, Zhekai Zhang, Muyang Li, Ligeng Zhu, Yao Lu, et al. Sana: Efficient high-resolution image synthesis with linear diffusion transformers. *arXiv preprint arXiv:2410.10629*, 2024. 3
- [56] Zhen Xiong, Yuqi Li, Chuanguang Yang, Tiao Tan, Zhihong Zhu, Siyuan Li, and Yue Ma. Enhancing image generation fidelity via progressive prompts. In *ICASSP 2025-2025 IEEE International Conference on Acoustics, Speech and Signal Processing (ICASSP)*, pages 1–5. IEEE, 2025. 3
- [57] XLabs-AI. x-flux. <https://github.com/XLabs-AI/x-flux>, 2024. 3, 6, 7
- [58] Zexuan Yan, Yue Ma, Chang Zou, Wenteng Chen, Qifeng Chen, and Linfeng Zhang. Eedit: Rethinking the spatial and temporal redundancy for efficient image editing. *arXiv preprint arXiv:2503.10270*, 2025. 3
- [59] Zhuoyi Yang, Jiayan Teng, Wendi Zheng, Ming Ding, Shiyu Huang, Jiazheng Xu, Yuanming Yang, Wenyi Hong, Xiaohan Zhang, Guanyu Feng, et al. Cogvideox: Text-to-video diffusion models with an expert transformer. *arXiv preprint arXiv:2408.06072*, 2024. 2
- [60] Yikuan Yuluo, Yue Ma, Kuan Shen, Tongtong Jin, Wang Liao, Yangpu Ma, and Fuquan Wang. Follow-your-shape: Shape-aware image editing via trajectory-guided region control. *arXiv preprint arXiv:2508.08134*, 2025. 3
- [61] Yikuan Yuluo, Yue Ma, Kuan Shen, Tongtong Jin, Wang Liao, Yangpu Ma, and Fuquan Wang. Gr-gaussian: Graph-based radiative gaussian splatting for sparse-view ct reconstruction. *arXiv preprint arXiv:2508.02408*, 2025. 3
- [62] Evelyn Zhang, Jiayi Tang, Xuefei Ning, and Linfeng Zhang. Training-free and hardware-friendly acceleration for diffusion models via similarity-based token pruning. In *Proceedings of the AAAI Conference on Artificial Intelligence*, pages 9878–9886, 2025. 3
- [63] Lvmin Zhang, Anyi Rao, and Maneesh Agrawala. Adding conditional control to text-to-image diffusion models. In *Proceedings of the IEEE/CVF international conference on computer vision*, pages 3836–3847, 2023. 2, 3
- [64] Richard Zhang, Phillip Isola, Alexei A Efros, Eli Shechtman, and Oliver Wang. The unreasonable effectiveness of deep features as a perceptual metric. In *Proceedings of the IEEE conference on computer vision and pattern recognition*, pages 586–595, 2018. 6

- [65] Yinhan Zhang, Yue Ma, Bingyuan Wang, Qifeng Chen, and Zeyu Wang. Magiccolor: Multi-instance sketch colorization. *arXiv preprint arXiv:2503.16948*, 2025. [3](#)
- [66] Chenyang Zhu, Kai Li, Yue Ma, Longxiang Tang, Chengyu Fang, Chubin Chen, Qifeng Chen, and Xiu Li. Instantswap: Fast customized concept swapping across sharp shape differences. *arXiv preprint arXiv:2412.01197*, 2024. [3](#)
- [67] Chenyang Zhu, Kai Li, Yue Ma, Chunming He, and Xiu Li. Multibooth: Towards generating all your concepts in an image from text. In *Proceedings of the AAAI Conference on Artificial Intelligence*, pages 10923–10931, 2025. [3](#)
- [68] Tianrui Zhu, Shiyi Zhang, Jiawei Shao, and Yansong Tang. Kv-edit: Training-free image editing for precise background preservation. *arXiv preprint arXiv:2502.17363*, 2025. [3](#)
- [69] Chang Zou, Xuyang Liu, Ting Liu, Siteng Huang, and Linfeng Zhang. Accelerating diffusion transformers with token-wise feature caching. *arXiv preprint arXiv:2410.05317*, 2024. [3](#), [7](#), [8](#)
- [70] Chang Zou, Evelyn Zhang, Runlin Guo, Haohang Xu, Conghui He, Xuming Hu, and Linfeng Zhang. Accelerating diffusion transformers with dual feature caching. *arXiv preprint arXiv:2412.18911*, 2024. [3](#), [8](#)